Supplementary Material of SupeRVol: Super-Resolution Shape and Reflectance Estimation in Inverse Volume Rendering

Mohammed Brahimi[1] Bjoern Haefner[1] Tarun Yenamandra[1] Bastian Goldluecke[2] Daniel Cremers[1]
[1] Technical University of Munich, [2] University of Konstanz
{mohammed.brahimi, bjoern.haefner, tarun.yenamandra, cremers}@tum.de
bastian.goldluecke@uni-konstanz.de

Abstract

In this supplementary material, we show further insight into SupeRVol. Specifically we describe the networks architecture with all its parameters and training specifications, we elaborate on the capturing process to retrieve the synthetic and real-world photometric images, we visualize the data set's input, and we show novel renderings with changed reflectance.

1. Network Details

1.1. Architecture

As mentioned in the main paper, we use three multilayer perceptrons (MLPs). One describes the geometry via an SDF, d_θ, one describes the BRDF's diffuse albedo, ρ_{γ_1}, and one is used for the specular parameters of the material, α_{γ_2}. The MLP of d_θ consists of 5 layers of width 512, with a skip connection at the 4-th layer. The MLPs of ρ_{γ_1} and α_{γ_2} consist of 4 layers of width 512, and 3 layers of width 256, respectively.
In order to compensate the spectral bias of MLPs [6], the input is encoded by positional encoding using 6 frequencies for both d_θ and α_{γ_2}, and 12 frequencies for ρ_{γ_1}.

1.2. Parameters and Cost Function

Similarly to [9, 10], we assume that the scene of interest lies within the unit sphere, which can be achieved by normalizing the camera positions appropriately. To approximate the Volume rendering integral (2) using (4), we use $m = 98$ samples which are also used to approximate (3), all with the sampling strategy of [8].
In the following, we distinguish between the ablation study noSR of the main paper and SupeRVol.
For SupeRVol, we set the objective's function trade-off parameters $\lambda_1 = \lambda_2 = 0.1$. Furthermore, in order to approximate the convolution with a Gaussian PSF (8), we use $N_s = 25$ in (9), and the terms of the objective function (10) and (11) consist of a batch size of 100 (inside the silhouette) and 1000, respectively. For the mask term (12) of the objective function, we use the same batch as (10), and add around 500 additional rays outside the silhouette whose rays still intersect with the unit sphere.
Concerning the noSR parameters, we set the objective's function trade-off parameters $\lambda_1 = 0.1$, $\lambda_2 = 0$, i.e. we *turn off* mask supervision, and the terms of the objective function (10) and (11) consist of a batch size of 2000 and 1000, respectively.
Note, that we always normalize each objective function's summand with its corresponding batch size.

1.3. Training

We train our networks using the Adam optimizer [3] with a learning rate initialized with $5\text{e}-4$ and decayed exponentially during training to $5\text{e}-5$, except for the MLP α_{γ_2} whose learning rate is constantly equal to $1\text{e}-5$. The remaining parameters are kept to Pytorch's default.
We train for 2000 epochs, which lasts about 2 days for noSR, and less than 3 days for SupeRVol using a single NVIDIA P6000 GPU with 24GB memory and 60 input images. For SupeRVol, we fix the geometry after the end of the training, and refine the BRDF's parameters using a larger batch size of 500 – all within the object's silhouette.

2. Data Acquisition

In this section we describe how we generated the data sets used in this paper

2.1. Synthetic Data

The synthetic data sets *dog1*, *dog2*, *girl1*, *girl2* were generated using Blender [2] and Matlab [5], where Blender [2] is used to render depth, normal and BRDF parameter maps for each viewpoint, and Matlab [5] is used to render images

using equation (6) and (7) of the main paper.
Exemplary low-resolution rendered images of size 320×240, as well as the object's GT high-resolution shape, diffuse albedo, roughness and specular albedo of size 1280×960 are shown in Figures 1–4, where the low-resolution images are obtained by blurring and downsampling high-resolution images by a factor 16 (four in each direction).

2.2. Real-World Data

The real-world data of *pony* was shared by the authors of [1], and the real-world data of *bird* was created by ourselves. We use a Samsung Galaxy Note 8 smartphone and the application "CameraProfessional"[1] to generate RAW images as well as the smartphone's images in parallel. We use the RAW images for our algorithm, and we pre-processed those using Matlab [5] by following [7], where we avoid non-linear operations such as gamma correction. Exemplary low-resolution images of both real-world datasets are shown in Figure 5, where *pony* (top) has a resolution of size 270×480 and *bird* (bottom) has a resolution of size 504×378. These $16\times$ (4 in each direction) downsampled low-resolution images are obtained similarly to synthetic data.

3. Novel Renderings

To validate that our approach results in the scene's parameters which can be used to alter the material and visualize it under novel illumination with standard software (Blender [2]), we show novel renderings in Fig. 6.

[1] https://play.google.com/store/apps/details?id=com.azheng.camera.professional, accessed 18-th Nov. 2022, 5.21PM

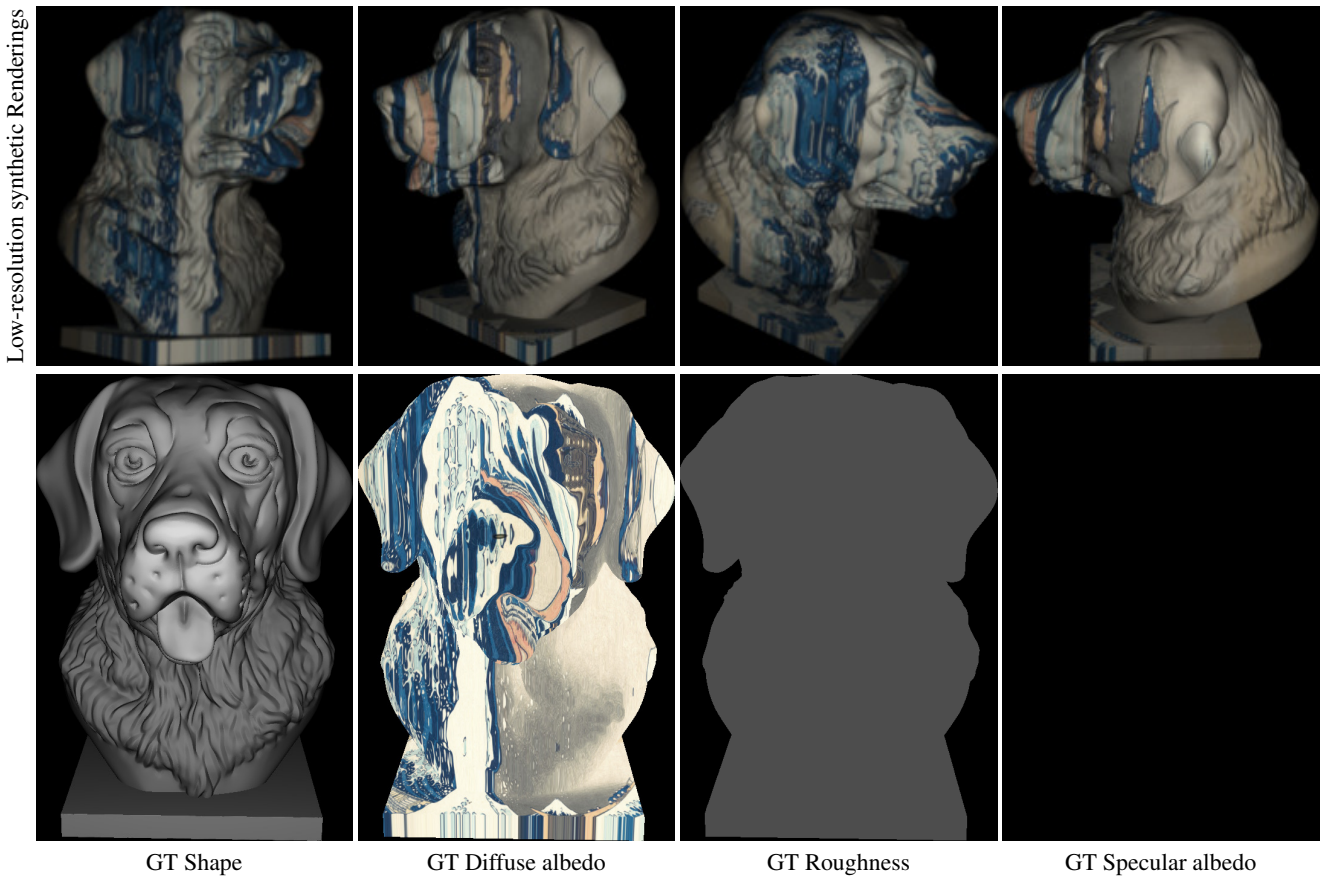

Figure 1. *dog1* dataset. Four example low-resolution images (top) and the GT's high-resolution shape, diffuse albedo, roughness and specular albedo (bottom).

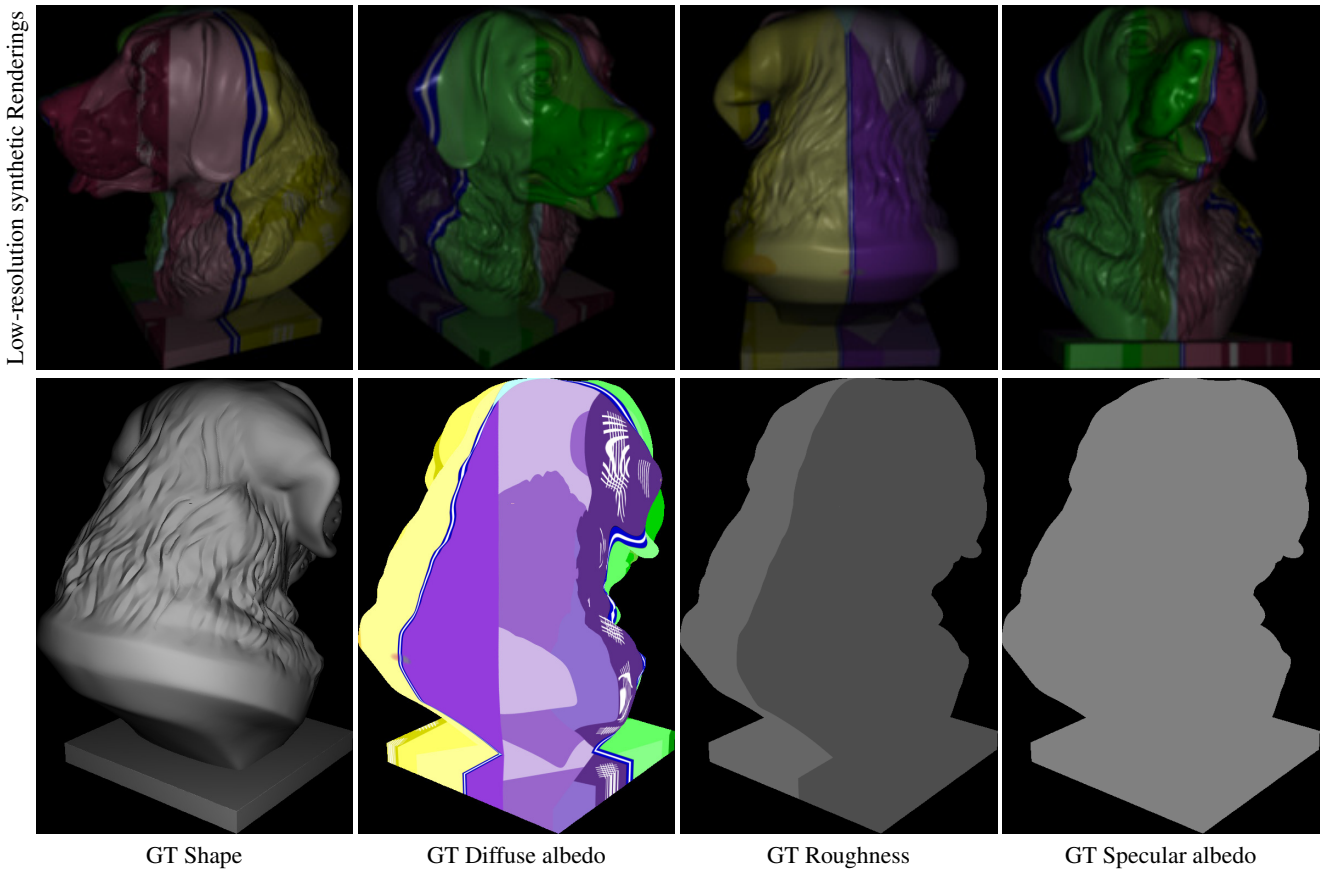

Figure 2. *dog2* dataset. Four example low-resolution images (top) and the GT's high-resolution shape, diffuse albedo, roughness and specular albedo (bottom).

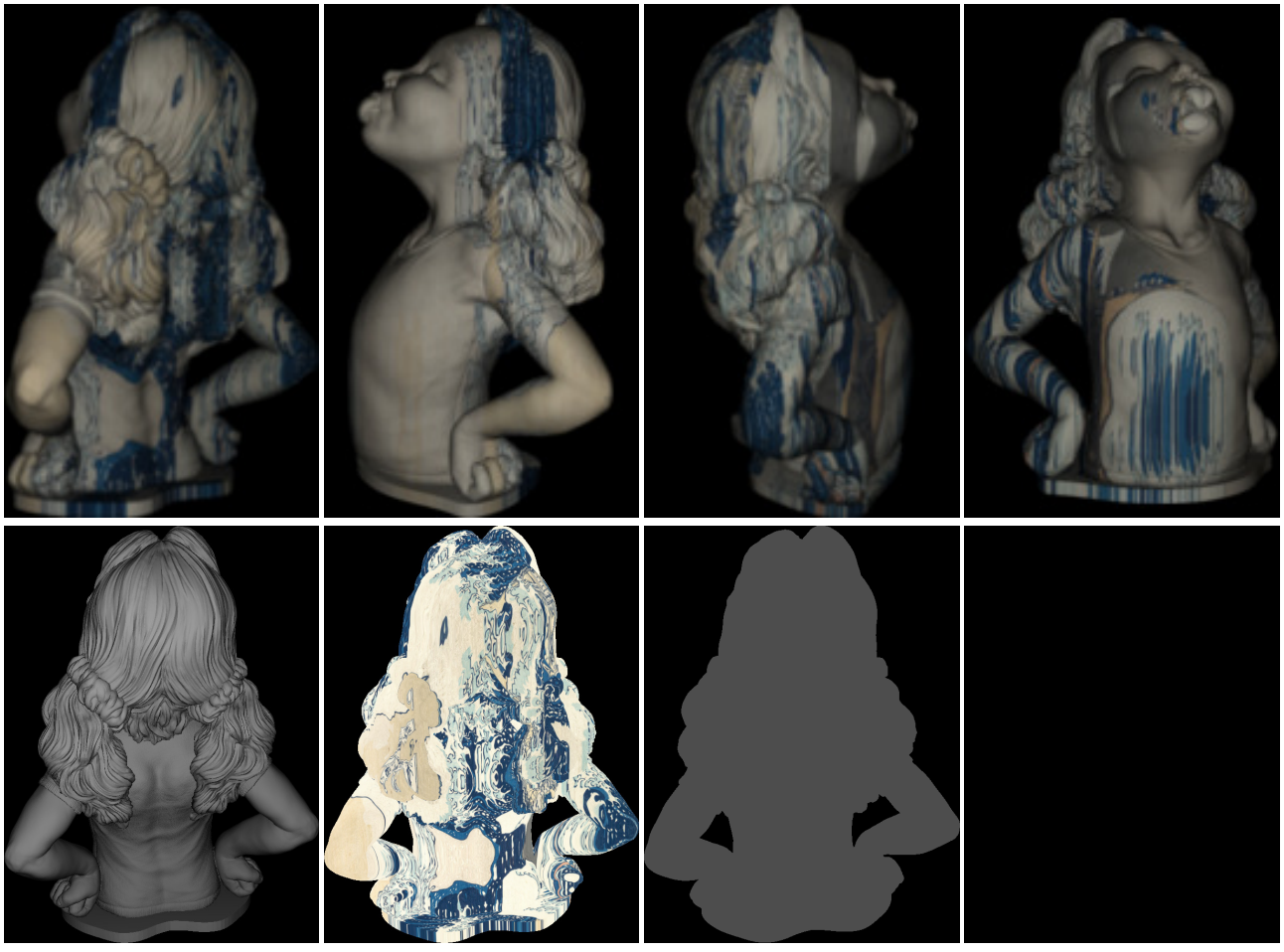

Figure 3. *girl1* dataset. Four example low-resolution images (top) and the GT's high-resolution shape, diffuse albedo, roughness and specular albedo (bottom).

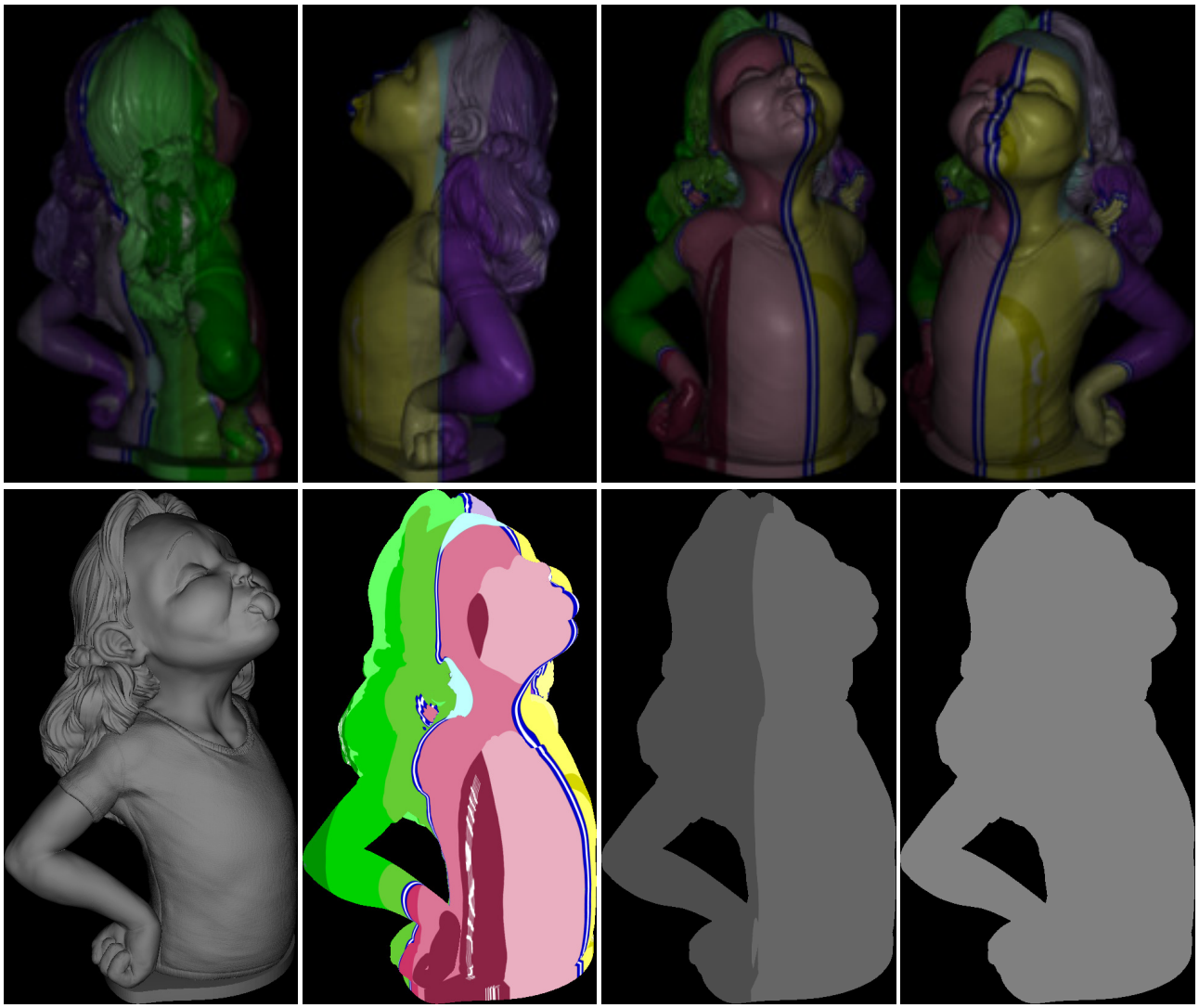

Figure 4. *girl2* dataset. Four example low-resolution images (top) and the GT's high-resolution shape, diffuse albedo, roughness and specular albedo (bottom).

Figure 5. Four low-resolution example images of the *bird* and *pony* dataset.

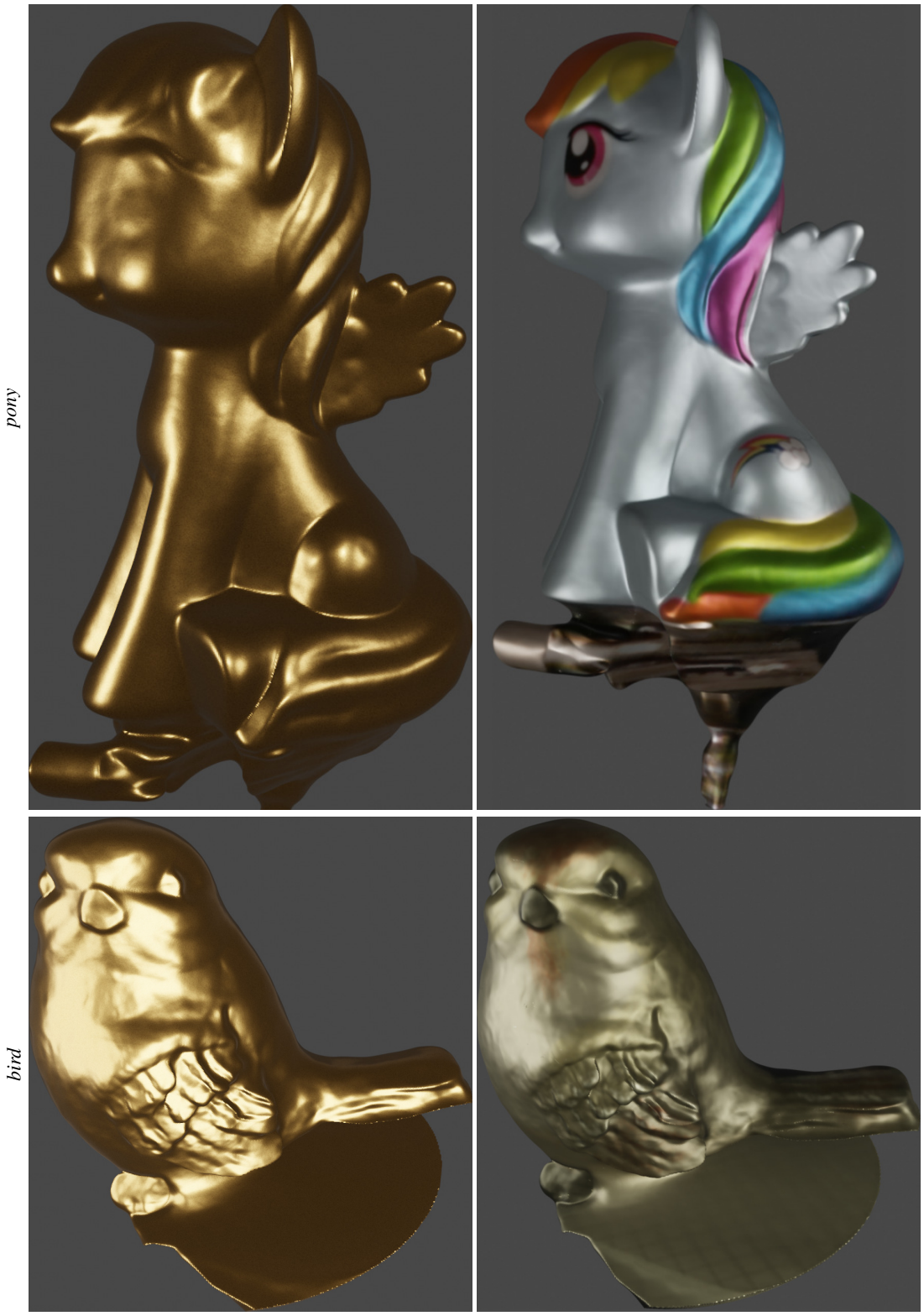

Figure 6. Novel rendering of *pony* and *bird* dataset. Both shapes where extracted from the learned sdf d using [4] and their BRDF was altered in Blender [2]. (left) shows a BRDF simulating gold, (right) uses the estimated diffuse albedo, with a more metallic, rougher and emissive material.

References

[1] Sai Bi, Zexiang Xu, Kalyan Sunkavalli, Miloš Hašan, Yannick Hold-Geoffroy, David Kriegman, and Ravi Ramamoorthi. Deep reflectance volumes: Relightable reconstructions from multi-view photometric images. In *European Conference on Computer Vision*, pages 294–311. Springer, 2020. 2

[2] Blender Online Community. *Blender - a 3D modelling and rendering package*. Blender Foundation, Stichting Blender Foundation, Amsterdam, 2018. 1, 2, 8

[3] Diederik P Kingma and Jimmy Ba. Adam: A method for stochastic optimization. *arXiv preprint arXiv:1412.6980*, 2014. 1

[4] William E. Lorensen and Harvey E. Cline. Marching cubes: A high resolution 3d surface construction algorithm. *SIGGRAPH Comput. Graph.*, 21(4):163–169, aug 1987. 8

[5] MATLAB. *version 9.8.0.1873465 (R2020a) Update 8*. The MathWorks Inc., Natick, Massachusetts, 2020. 1, 2

[6] Ben Mildenhall, Pratul P Srinivasan, Matthew Tancik, Jonathan T Barron, Ravi Ramamoorthi, and Ren Ng. Nerf: Representing scenes as neural radiance fields for view synthesis. *Communications of the ACM*, 65(1):99–106, 2021. 1

[7] Rob Sumner. Processing raw images in matlab. *Department of Electrical Engineering, University of California Sata Cruz*, 2014. 2

[8] Lior Yariv, Jiatao Gu, Yoni Kasten, and Yaron Lipman. Volume rendering of neural implicit surfaces. *Advances in Neural Information Processing Systems*, 34:4805–4815, 2021. 1

[9] Lior Yariv, Yoni Kasten, Dror Moran, Meirav Galun, Matan Atzmon, Basri Ronen, and Yaron Lipman. Multiview neural surface reconstruction by disentangling geometry and appearance. *Advances in Neural Information Processing Systems*, 33:2492–2502, 2020. 1

[10] Kai Zhang, Fujun Luan, Zhengqi Li, and Noah Snavely. Iron: Inverse rendering by optimizing neural sdfs and materials from photometric images. In *Proceedings of the IEEE/CVF Conference on Computer Vision and Pattern Recognition*, pages 5565–5574, 2022. 1